Surgery 165 (2019) 1168–1175

Contents lists available at ScienceDirect

Surgery

journal homepage: www.elsevier.com/locate/surg

Predictive model for microvascular invasion of hepatocellular carcinoma among candidates for either hepatic resection or liver transplantation

Hidetoshi Nitta, MD, PhD, FACS[a,b,*], Marc-Antoine Allard, MD[a], Mylène Sebagh, MD[c], Vincent Karam, PhD[a], Oriana Ciacio, MD[a], Gabriella Pittau, MD[a], Eric Vibert, MD, PhD[a], Antonio Sa Cunha, MD[a], Daniel Cherqui, MD[a], Denis Castaing, MD[a], Henri Bismuth, MD, PhD[a], Catherine Guettier, MD, PhD[d], Didier Samuel, MD, PhD[a], Hideo Baba, MD, PhD, FACS[b], René Adam, MD, PhD[a]

[a] Centre Hépato-Biliaire, AP-HP, Hôpital Paul Brousse, Université Paris-Sud, Inserm U 935 and U 1193, Villejuif, France
[b] Departement of Gastroenterological Surgery, Graduate School of Life Sciences, Kumamoto University, Japan
[c] Departement of Pathology, Hôpital Paul Brousse, Assistance Publique-Hôpitaux de Paris, Villejuif, France
[d] Departement of Pathology, Bicêtre University Hospital, Université Paris-Sud, Le Kremlin-Bicêtre, Ile-de-France, France

ARTICLE INFO

Article history:
Accepted 21 January 2019
Available online 14 March 2019

ABSTRACT

Background: Microvascular invasion is the strongest prognostic factor of survival in patients with hepatocellular carcinoma. We therefore developed a predictive model for microvascular invasion of hepatocellular carcinoma to help guide treatment strategies in patients scheduled for either hepatic resection or liver transplantation.

Methods: Patients with hepatocellular carcinoma who underwent hepatic resection or liver transplantation from 1994 to 2016 were divided into training and validation cohorts. A predictive model for microvascular invasion was developed based on microvascular invasion risk factors in the training cohort and validated in the validation cohort.

Results: A total of 910 patients (425 having received hepatic resection, 485 having received liver transplantation) were included in the training ($n = 637$) and validation ($n = 273$) cohorts. Multivariate analysis identified α-fetoprotein ≥100 ng/mL (relative risk 3.05, $P < .0001$), tumor size ≥40 mm (relative risk 1.98, $P = .0002$), nonboundary hepatocellular carcinoma type (relative risk 1.91, $P = .001$), neutrophil-to-lymphocyte ratio (relative risk 1.86, $P = .002$), and aspartate aminotransferase (relative risk 1.53, $P = .02$) as associated with microvascular invasion. The estimated probability of microvascular invasion ranged from 17.0% in patients with none of these factors to 86.9% in the presence of all factors. This model achieved a C-index of 0.732 in the validation cohort. The 5-year overall survival of patients with ≥50% probability of microvascular invasion was poorer than that of patients with <50% probability (hepatic resection; 39.1% vs 61.2%, $P < .0001$, liver transplantation; 5-year overall survival, 54.8% vs 79.0%, $P = .05$).

Conclusion: This model developed from preoperative data allows reliable prediction of microvascular invasion in candidates for either hepatic resection or liver transplantation.

Introduction

Microvascular invasion (MVI) of hepatocellular carcinoma (HCC) is a significant poor prognostic factor of survival in patients undergoing hepatic resection (HR) and liver transplantation (LT),[1–4] and a better predictor of tumor recurrence and overall survival (OS) than the commonly used Milan criteria.[5] However, MVI is only diagnosed by pathologic examination after HR or LT and is impossible to predict preoperatively. Given that the probability of preoperative MVI may influence the choice of surgical strategy, it is necessary to develop a more accurate predictive model for MVI.

Advanced [^{18}F]-fluorodeoxyglucose positron emission tomography or diffusion-weighted magnetic resonance imaging (MRI) images and genetic markers may help to predict MVI.[6–9] However, studies of these techniques have included limited numbers of

* Reprint requests: Hidetoshi Nitta, Centre Hépato-Biliaire, 9 Avenue Paul Vaillant Couturier, 94804 Villejuif, France. Tel: +33 1 45 59 30 49; Fax: +33 1 45 59 38 57.
E-mail address: hnitta5085@gmail.com (H. Nitta).

https://doi.org/10.1016/j.surg.2019.01.012
0039-6060/

patients, and furthermore, the costs and expertise required by these techniques may inhibit their routine use. A predictive model of MVI based on easily available factors and imaging techniques may thus offer a more practical and useful approach.

Treatment strategies take into consideration the patient's general condition, tumor status, and liver function.[10,11] HR is generally considered when the tumor status and liver function are favorable, and LT may be preferred when the liver function is unfavorable and tumor status less advanced. Most risk models for MVI are adapted for either HR or LT,[2] but not all patients can be clearly assigned to one of these approaches because of their background, tumor status, liver function, and the organ shortage. A predictive model for MVI that could be used to guide treatment strategies in patients scheduled for either HR or LT would therefore be a valuable tool. This study therefore aimed to identify independent predictors of MVI and establish a user-friendly model to predict MVI based on preoperative factors in candidates for either HR or LT. We then sought to assess the value of our model in a validation cohort.

Patients and Methods

Patient population

We included 1,051 consecutive patients diagnosed with HCC preoperatively, who underwent HR ($n = 490$) or LT ($n = 561$) at the Paul Brousse Hospital, Villejuif, France, between January 1994 and June 2016. We excluded patients who were diagnosed as not having HCC by pathologic examination ($n = 74$), having undergone R2 resection ($n = 5$), having had macrovascular invasion ($n = 48$), or providing insufficient data ($n = 14$). The remaining 910 patients were included in the study. Patients diagnosed with HCC preoperatively were included, even if they underwent pretreatment before HR or LT. Patients who underwent surgery between January 1994 and June 2012 were assigned to the training cohort ($n = 637$), and those who underwent surgery between July 2012 and May 2016 were assigned to the validation cohort ($n = 273$). The median follow-up time for the training cohort was 86.3 months (HR patients, 59.0 months; LT patients, 116.5 months).

Preoperative diagnosis and treatment

HCC diagnosis was based on imaging data (ultrasound, contrast-enhanced computed tomography [CE-CT], and MRI), serum α-fetoprotein (AFP), and clinical parameters according to recent international guidelines.[12] The optimal treatment strategies for HCC patients were determined at multidisciplinary meetings involving surgeons, oncologists, hepatologists, and radiologists. Patients with multiple tumors with unpreserved liver function or severe portal hypertension were proposed for LT, as described elsewhere.[13]

Clinical parameters

All clinical parameters, including hematologic and biochemical findings and tumor markers, were obtained within 1 month before surgery. The largest tumor size and tumor number preoperatively were based on preoperative CE-CT. For patients who underwent pretreatment, the clinical parameters and the radiologic images were obtained at the latest date before surgery after pretreatment. The largest tumor gross shape was evaluated by experienced radiologists based on CE-CT and classified into one of four types based on gross morphologic appearance. Tumor shapes that were not evaluable by CE-CT because of lipiodol deposition after transcatheter arterial chemoembolization (TACE) were evaluated by MRI. The types were defined as follows:

- Type 1—single nodular type with round or oval shape with a clear boundary, with or without fibrous pseudocapsule;
- Type 2—single nodular type with extranodular growth roughly resembling type 1 but with varying degrees of local extranodular growth;
- Type 3—confluent multinodular type encompassing a cluster of small and confluent nodules, each with a clear margin or capsule, and the tumor lobulated as a whole; and
- Type 4—infiltrative type with irregular shape and unclear border.[14,15]

We defined type 1 as boundary type and types 2–4 as non-boundary types.

Pathologic examination

All pathologic specimens were routinely examined by two pathologists (C.G. and M.S.) who were experts in liver tumor pathology. Specimens were cut into 5-mm thick slices. For tumors < 2 cm, nodules were sampled in their entirety. For larger lesions, nodules were sampled extensively from the center to the periphery, with the number of samples at the discretion of the pathologist. Sections were stained with hematoxylin-eosin-saffron. MVI was defined when cancer cells were present within the lumens of veins and venules. In the event of any uncertainty, tumoral invasion was confirmed by immunohistochemistry using a vascular antibody (CD34, D240).

Statistical analysis

Categorical variables were compared using χ^2 or the Fisher exact tests. Continuous variables were shown as mean ± standard deviation and compared using Mann-Whitney *U* tests. Cutoff values for continuous factors were determined based on receiver-operating characteristic (ROC) curve analysis.

No data were missing for most variables among the training cohort, except hepatitis B virus-DNA (n =16, 2.5%), hepatitis C virus-RNA ($n = 78$, 12.2%), body mass index ($n = 19$, 3.0%), platelet count ($n = 8$, 1.3%), albumin ($n = 37$, 5.8%), neutrophil-to-lymphocyte ratio ([NLR] $n = 35$, 5.5%), creatinine ($n = 6$, 0.9%), gamma-glutamyltransferase ($n = 11$, 1.7%), alkaline phosphatase ([ALP] $n = 27$, 4.2%), alanine aminotransferase ([ALT] ($n = 2$, 0.3%), and boundary type on CT ($n = 90$, 14.1%). The exclusion of patients with missing data might lead to biased risk estimates,[16,17] and multiple imputation ($N = 20$) was therefore performed for all multivariate analyses, using the R package (mice). No data were missing in the validation cohort. Each of the imputed data sets ($n = 20$) was analyzed separately using a multivariable Cox regression or logistic regression model and pooled to identify independent predictors of survival or MVI, respectively. Variables with a $P < .20$ in univariate analysis were subjected to multivariate analysis using Cox proportional hazards and logistic regression models. All variables associated with prognosis and MVI were candidates, using a stepwise backward elimination procedure with a threshold of $P < .05$. The level of significance for all tests was set at $P < .05$. The probabilities of MVI in the predictive model were calculated based on the coefficients obtained in the multivariate logistic regression model. The predictive performance of the model was measured by the concordance index (C-index) and calibration with 400 bootstrap samples. Cumulative OS and recurrence-free survival (RFS) curves were obtained using the Kaplan–Meier method. The OS and RFS rates after surgery were estimated by the log-rank test. Survival time was calculated from the date of HR or LT to the date of the event of interest, or the date of last follow-up. To estimate RFS, patients with no evidence of recurrence were censored at the time

Table I
Multivariate analysis of prognostic factors for overall and recurrence-free survival among patients who underwent hepatic resection or transplantation (Cox proportional hazard model)

	Hazard ratio	95% CI	*P* value
Hepatic resection OS			
Tumor number >3	2.73	1.14–5.52	.03
MVI	2.63	1.72–4.05	< .0001
Albumin <35 g/l	1.82	1.21–2.76	.004
Hepatic resection RFS			
Tumor number > 3	2.77	1.35–5.01	.007
MVI	1.98	1.44–2.70	< .0001
Transplantation OS			
MVI	2.35	1.69–3.27	< .0001
Age ≥ 52 years	1.67	1.13–2.56	.01
Tumor size ≥ 40 mm	1.52	1.06–2.16	.02
Transplantation RFS			
Tumor size ≥ 40 mm	4.43	2.40–8.17	< .0001
MVI	3.22	1.73–6.17	.0002
Nonboundary type	1.77	1.02–3.25	.04

CI, confidence inverval; *OS*, overall survival; *RFS*, recurrence-free survival; *MVI*, microvascular invasion.
Note: The following variables were subjected to univariate analysis: age, sex, body mass index, diabetes, alcohol, HBs-Ag, HBV-DNA, HCV-Ab, HCV-RNA, Child–Pugh, MELD score, platelet count, albumin, total bilirubin, prothrombin time–international normalized ratio, creatinine, AST, ALT, gamma-glutamyltransferase, ALP, NLR, alfa-fetoprotein, tumor size, tumor number, transfusion, nonboundary type, tumor differentiation, MVI, satellite lesion, tumor capsulation, and surgical margin.

of last follow-up or death. All statistical analyses were performed using JMP ver.12 (SAS Institute, Cary, NC, USA), R v 3-1.1.

Results

Risk factors for prognosis in training cohort and outcomes with or without microvascular invasion

The backgrounds of the patients in the training and validation cohorts are presented in Supplementary Table I. We initially evaluated the risk factors for poor OS and RFS among the training cohort (Table I). In patients who underwent HR, MVI was an independent risk factor for OS (hazard ratio 2.63; 95% confidence interval [CI], 1.72–4.05; $P < .0001$) and RFS (hazard ratio 1.98; 95% CI, 1.44–2.70; $P < .0001$). MVI was also an independent risk factor for OS (hazard ratio 2.35; 95% CI, 1.69–3.27; $P < .0001$) and RFS (hazard ratio 3.22; 95% CI, 1.73–6.17; $P = 0.0002$) in patients who underwent LT. The Kaplan–Meier curve according to MVI is presented in Figure 1. The 5-year OS and RFS in patients who underwent HR were significantly different with and without MVI (OS, 38.4% vs 66.1%, $P < .0001$; RFS, 15.8% vs 28.6%, $P < .0001$, respectively). The 5-year OS and RFS in patients who underwent LT with and without MVI were 51.4% vs 80.6% and 60.9% vs 89.9%, respectively (OS, $P < .0001$; RFS, $P < .0001$).

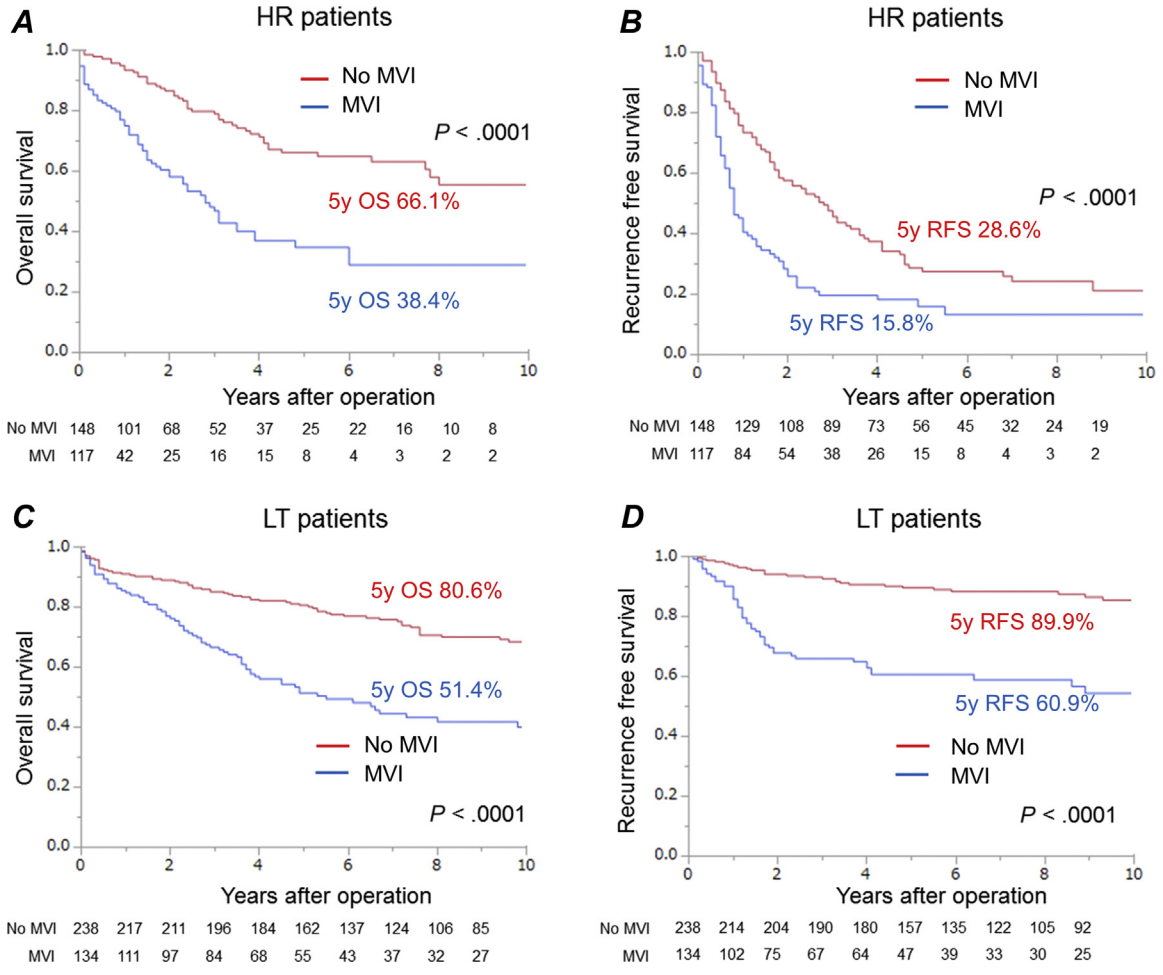

Fig 1. Overall survival curves for HCC patients who underwent (*A*) HR or (*C*) LT, stratified according to the presence or absence of MVI. Recurrence-free survival curves for HCC patients who underwent (*B*) HR or (*D*) LT, stratified according to the presence or absence of MVI.

Table II
Univariate and multivariate analyses of preoperative risk factors for microvascular invasion in the training cohort

		Univariate analysis			Multivariate analysis		
		No MVI ($n = 386$) Number, (%)	MVI ($n = 251$) Number, (%)	*P* value	RR	95% CI	*P* value
Sex	Male	320 (82.9)	216 (86.1)	.24			
	Female	66 (17.1)	35 (13.9)				
Age	≥ 52 years	309 (80.0)	188 (74.9)	.13	n.s.		
HBs-Ag	+	59 (15.8)	40 (16.3)	.82			
HBV-DNA	≥ 4 log	5 (1.3)	9 (3.7)	.06	n.s.		
HCV-Ab	+	142 (36.8)	100 (39.8)	.44			
HCV-RNA	Positive	59 (18.1)	52 (22.3)	.22			
Cirrhosis	+	60 (15.5)	43 (17.1)	.60			
Child-Pugh	A	213 (56.5)	129 (54.2)	.31			
	B	134 (35.5)	96 (40.3)				
	C	30 (8.0)	13 (5.5)				
MELD score	≥ 10	133 (34.7)	84 (33.6)	.77			
Body mass index	≥ 25	202 (54.2)	122 (49.8)	.30			
Alcohol	+	100 (25.9)	53 (21.1)	.16	n.s.		
Diabetes	+	101 (26.2)	74 (29.4)	.36			
Previous TACE	+	256 (66.3)	146 (58.2)	.04	n.s.		
Previous LAT	+	56 (14.5)	30 (12.0)	.35			
Previous HR	+	19 (4.9)	18 (7.2)	.24			
Platelet ($\times 10^4/\mu l$)	> 23	50 (13.1)	62 (25.0)	.0002	n.s.		
Total bilirubin (μmol/L)	≥ 18	212 (55.1)	133 (53.0)	.61			
Albumin (g/L)	≥ 35	159 (43.4)	83 (35.4)	.05	n.s.		
PT-INR	≥ 1.30	181 (46.9)	102 (40.6)	.12	n.s.		
NLR	≥ 3.2	89 (24.3)	91 (38.7)	.0002	1.86	1.26-2.75	.002
Creatinine (μmol/l)	≥ 113	37 (9.6)	31 (12.3)	.27			
GGT (U/L)	≥ 79	225 (59.1)	159 (64.9)	.14	n.s.		
ALP (U/L)	≥ 122	128 (35.0)	108 (44.3)	.02	n.s.		
AST (U/L)	≥ 62	148 (38.3)	130 (51.8)	.0008	1.53	1.08-2.17	.02
ALT (U/L)	≥ 40	194 (50.5)	146 (58.2)	.06	n.s.		
AFP (ng/mL)	≥ 100	45 (11.9)	82 (33.1)	< .0001	3.05	1.98-4.70	< .0001
Image results							
Largest tumor size in image (mm)	≥ 40	116 (30.0)	133 (53.0)	< .0001	1.98	1.38-2.84	.0002
Tumor number in image	≥ 2	168 (43.5)	106 (42.2)	.75			
Tumor number in image	> 3	28 (7.2)	33 (13.1)	.01	n.s.		
Nonboundary type	Yes	98 (29.4)	112 (52.3)	< .0001	1.91	1.29-2.82	.001

HBs-Ag, hepatitis B surface antigen; *HCV-ab*, hepatitis C virus antibody; *TACE*, transcatheter arterial chemoembolization; *LAT*, local ablation therapy; *PT-INR*, prothrombin time–international normalized ratio; *GGT*, gamma-glutamyltransferase; *ALT*, alanine aminotransferase; *AFP*, α-fetoprotein.

Preoperative risk factors for MVI after HR or LT in the training cohort

All variables in this univariate analysis were based on data obtained preoperatively. Univariate analysis identified 9 preoperative factors associated with MVI after HR and LT: previous transcatheter arterial chemoembolization, platelet count, NLR, ALP, aspartate aminotransferase [AST], AFP, largest tumor size on preoperative imaging, tumor number on preoperative imaging >3, and nonboundary type (Table II). Multivariate analysis identified 5 independent predictors for MVI: AFP ≥100 ng/mL (relative risk [RR], 3.05; 95% CI, 1.98–4.70; $P < .0001$), largest tumor size in image ≥ 40 mm (RR, 1.98; 95% CI, 1.38–2.84; $P = .0002$), nonboundary type (RR, 1.91; 95% CI, 1.29–2.82; $P = .001$), NLR ≥ 3.2 (RR, 1.86; 95% CI, 1.26–2.75; $P = .002$), and AST ≥62 (RR, 1.53; 95% CI, 1.08–2.17; $P = .02$ [Table II]). In addition, the predictive factors of MVI for each group underwent HR or LT, and patients without cirrhosis are presented in Supplementary Table II.

Development and validation of predictive model for MVI using training cohort

The predictive model was then developed using the 5 factors based on logistic regression analysis (Table III). The estimated probabilities (%) for MVI were thus weighted according to the RR for each of the 5 factors. The estimated probability of MVI was 17.0% in patients without any factors and increased to 86.9% in the presence of all factors. This predictive model was validated internally in the training cohort using the bootstrap validation method, with a bootstrap-corrected C-index of 0.710. In addition, calibration plots for the probability of MVI showed good calibration for the presence of MVI between the risk estimation according to the model and histopathologic confirmation in surgical specimens (Fig 2, *A*).

Validation of the predictive model for MVI using the validation cohort

The model was subsequently validated using the validation cohort. A calibration plot for the probability of MVI showed good calibration between the model's predicted and actual observations (unadjusted C-index 0.750; 95% CI, 0.683–0.805; bootstrap-corrected C-index 0.732) (Fig 2, *B*). When the validation cohort was divided into patients who underwent HR and those who underwent LT, the bootstrap-corrected C-indexes were 0.691 and 0.798, respectively, indicating good concordances in both groups (Figs 2, *C* and *D*). Moreover, when the validation cohort was divided into patients within and beyond the Milan criteria, the bootstrap-corrected C-indexes were 0.749 and 0.796, respectively (Supplementary Figs 1, *A* and *B*). The C-index of Child–Pugh A and B or C were 0.759 and 0.760, respectively (Supplementary Figs 1, *C* and *D*).

The relationships between MVI probabilities and actual MVI rates confirmed by pathologic examination are summarized in Table IV. The MVI probabilities corresponded closely with the actual MVI rates.

Outcomes of patients with high or low MVI probabilities

We evaluated the outcomes of HCC patients according to MVI probability in the training cohort. The optimal cutoff value for

Table III
Predictive model for microvascular invasion based on multivariate logistic regression analysis

Number of positive factors	AFP ≥ 100	Tumor size ≥40	Nonboundary type	NLR ≥ 3.2	AST ≥ 62	MVI probability (%)
5	+	+	+	+	+	86.9
4	+	+	+	+	−	81.4
	+	+	+	−	+	78.3
	+	+	−	+	+	77.7
	+	−	+	+	+	77.1
	−	+	+	+	+	68.3
3	+	+	+	−	−	70.4
	+	+	−	+	−	69.6
	+	−	+	+	−	68.9
	+	+	−	−	+	65.5
	+	−	+	−	+	64.7
	+	−	−	+	+	63.8
	−	+	+	+	−	58.7
	−	+	+	−	+	54.0
	−	+	−	+	+	53.0
	−	−	+	+	+	52.3
2	+	+	−	−	−	55.5
	+	−	+	−	−	54.7
	+	−	−	+	−	53.7
	+	−	−	−	+	49.0
	−	+	+	−	−	43.6
	−	+	−	+	−	42.6
	−	−	+	+	−	41.9
	−	+	−	−	+	38.1
	−	−	+	−	+	37.3
	−	−	−	+	+	36.4
1	+	−	−	−	−	38.7
	−	+	−	−	−	28.8
	−	−	+	−	−	28.2
	−	−	−	+	−	27.4
	−	−	−	−	+	23.8
0	−	−	−	−	−	17.0

MVI probability was 49.0% according to ROC analysis (area under the curve, 0.721). We therefore compared the prognoses of patients with MVI probabilities <50% and ≥50%. Among patients who underwent HR, the 5-year OS and RFS rates in patients with MVI probability ≥ 50% were significantly lower than those of patients with MVI probability <50% (5-year OS, 39.1% vs 61.2%, $P <$ .0001; 5-year RFS, 20.1% vs 24.7%, $P <$ .0001 [Figs 3, *A* and *B*]). Among patients who underwent LT, there was no significant difference in OS between patients with MVI probabilities ≥50% and <50% (5-year OS, 54.8% vs 79.0%, $P = .05$), but the 5-year RFS in patients with an MVI probability ≥50% was significantly poorer than in patients with an MVI probability <50% (5-year RFS, 61.2% vs 88.2%, $P <$ .0001) (Figs 3, *C* and *D*). When the training cohort was divided into patients within and beyond the Milan criteria, the outcomes of patients with an MVI probability ≥50% was worse than that of patients with MVI probability <50% (Supplementary Fig 2).

Comparison of predictive powers

The predictive powers of MVI in our predictive model, the other predicting model (artificial neural network[18]), and the LT criteria (Milan criteria, University of California at San Francisco criteria and AFP model[19]) were compared by ROC curve analysis in the validation cohort. The area under the ROC curve of our model was significantly better than those of the other models among either patients who underwent HR or patients who underwent LT (Supplementary Fig 3).

Discussion

The results of this study showed that the risk of death or recurrence in patients with MVI, which accounted for about 40% of all patients, was two to three times higher than in patients without MVI who underwent HR or LT. Preoperative evaluation of the probability of MVI could thus influence the choice of surgical strategy. Multivariate analysis identified 5 preoperative factors that were significantly associated with the presence of MVI: AFP ≥ 100 ng/mL, nonboundary type in CE-CT, NLR ≥ 3.2, AST ≥ 62, and largest tumor size in CE-CT ≥40 mm. The predictive model suggested that the probability of MVI varied from 17.0% to 86.9%, depending on the combinations of these 5 factors. The performance of this model was supported by C-index values of 0.710 and 0.732 in the training and validation cohorts, respectively, and by optimal calibration curves demonstrating agreement between the predicted and actual observations. Moreover, the predictive power for MVI of the model was significantly better than those of the other MVI predicting model and LT criteria.

Some studies have attempted to predict MVI, but most had some limitations, such as having small sample sizes and being limited to patients with early HCC or hepatitis B antigen-related HCC,[2,20] thus limiting the general use of these models in all HCC patients. In contrast, the current study included all patients diagnosed with HCC preoperatively, and thus included patients with various tumor characteristics and liver functions. The current study analyzed common data sets for patients who underwent HR or LT because not all patients with HCC can be clearly assigned to one of these approaches. The resulting predictive model demonstrated high accuracy in patients with Child–Pugh A (C-index, 0.759), B or C (C-index, 0.760) among the validation cohort, suggesting that it could be adopted for patients with or without cirrhosis. Moreover, the high C-indexes for patients within (0.749) and beyond the Milan criteria (0.796) also suggested that the predictive model was suitable for both groups. Furthermore, the high C-indexes in patients who underwent LT (0.798) and HR (0.691) suggested that the model may be useful for

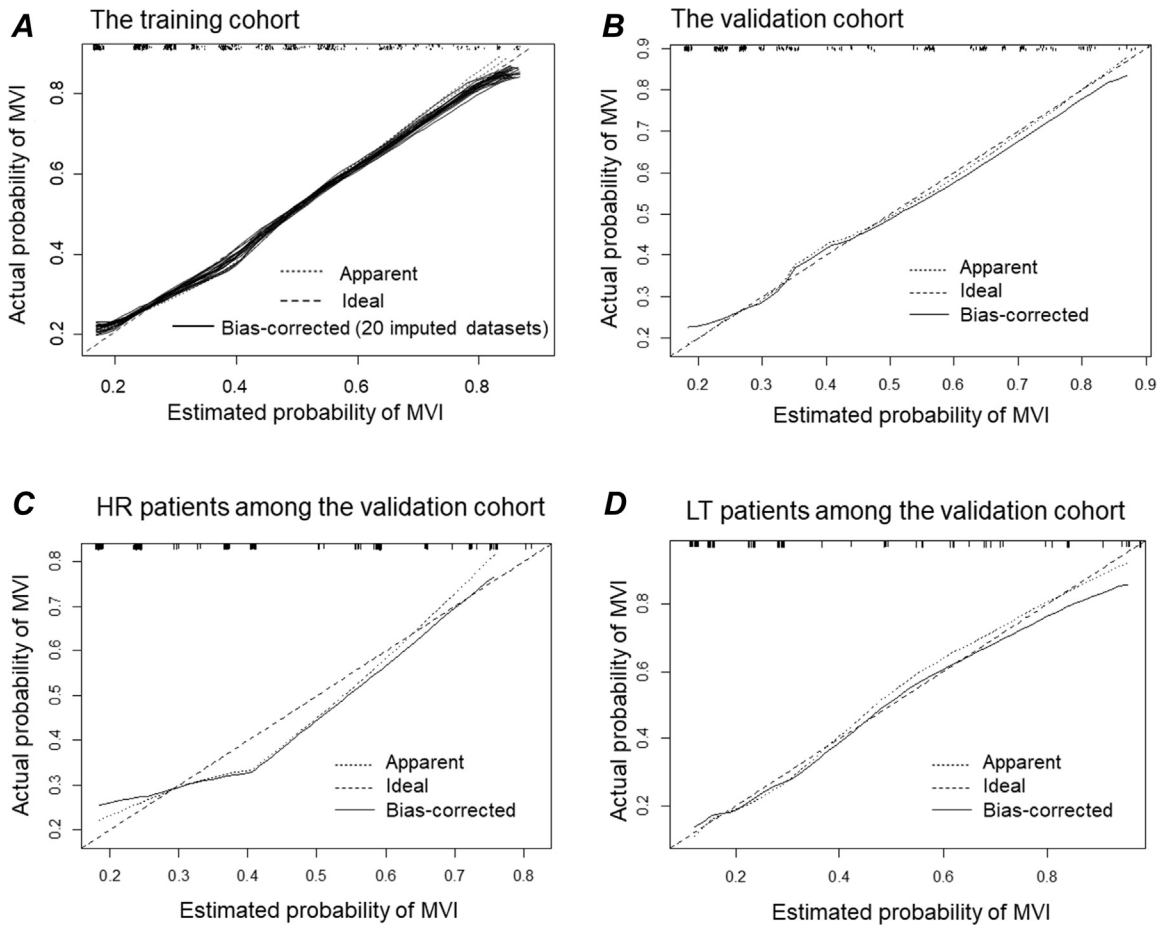

Fig 2. Calibration plots comparing predicted and actual MVI probabilities among (*A*) the training cohort, (*B*) the validation cohort, (*C*) HR patients in the training cohort, and (*D*) transplantation patients in the training cohort. The *dotted line* indicates the ideal prediction and the *solid line* is the bias-corrected prediction with 400 bootstraps.

Table IV
Relationship between MVI probability based on the model and actual MVI rate

MVI probability, %	Training cohort		Validation cohort		Total cohort	
	Actual MVI rate, %	*P* value	Actual MVI rate, %	*P* value	Actual MVI rate, %	*P* value
≤ 30	22.4 (56/250)	.001*	24.5 (37/151)	.0009*	23.2 (93/401)	< .0001*
> 30–50	37.8 (51/135)	.0002†	47.1 (32/68)	.30†	40.9 (83/203)	.0001†
> 50–70	63.6 (63/99)	.17‡	57.5 (23/40)	.02‡	61.9 (86/139)	.02‡
> 70	75.0 (36/48)		92.9 (13/14)		79.0 (49/62)	

* ≤30 vs >30–50.
† >30–50 vs >50–70.
‡ >50–70 vs >70.

helping to determine the optimal treatment strategy in both groups of patients.

In addition to tumor size and number, MVI should also be considered when choosing a surgical strategy because this is one of the strongest factors predicting poor prognosis among patients undergoing HR or LT, even within the Milan criteria.[5,21,22] The prognosis of patients with MVI who underwent LT was poor (5-year OS, 51.4%; 5-year RFS, 60.9%). Therefore, it may be better to avoid upfront LT for patients who are more likely to have MVI, not only because of the poor prognosis but also because of the current organ shortage. The cutoff value based on MVI probability was 50% according to ROC analysis. This cutoff value could be an important clinical indicator for deciding on the treatment strategy for HCC. The outcomes of LT in patients with high MVI probability (≥ 50%) were poor (5-year OS: 49.7%; 5-year RFS: 48.0%), suggesting that these patients should not be considered for upfront LT. AFP was the strongest risk factor for MVI in our study. If locoregional therapy can reduce the AFP value to less than 100 ng/mL without exacerbating other factors (tumor size, tumor shape, NLR, and AST), the probability of MVI will be reduced, as presented in Table III. Halazun et al[23] reported that the AFP response to locoregional therapies before LT was an independent predictor of RFS. Therefore, for patients with a high MVI probability, the decrease in the MVI probability after locoregional therapy before LT may be important in selecting good candidates for LT, and this may lead to an improved prognosis. Patients with a ≥50% probability of MVI among patients who underwent HR showed significantly poorer prognoses than those with <50% probability (5-year OS: 42.4% vs 56.7%, $P = .001$). No consensus exists on how to undergo HR for HCC with MVI. However, in this study, the rate of microsatellite lesions in patients with MVI was 47% (118 of 251), which was significantly higher than for patients without MVI (23%, 89 of 386) ($P < .0001$, *data not*

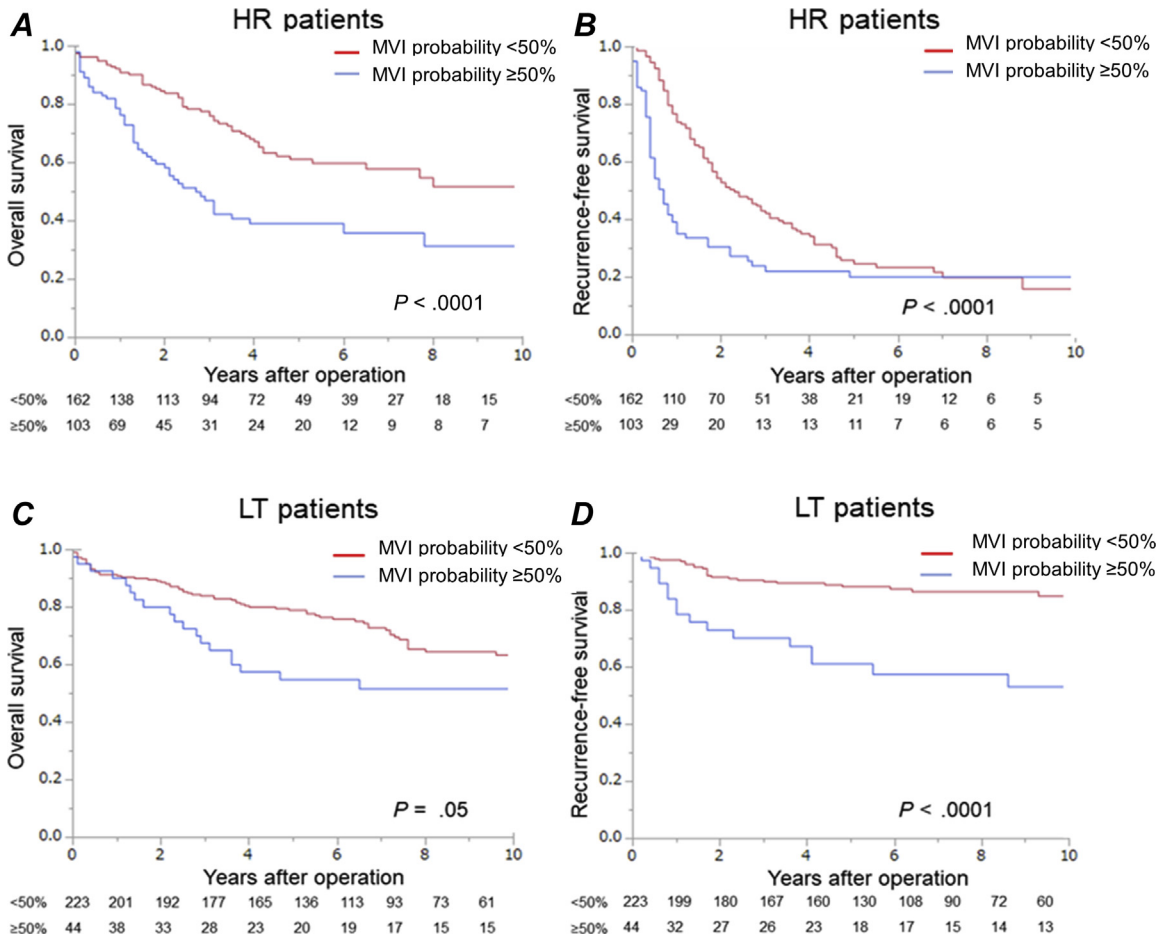

Fig 3. (*A*) Overall and (*B*) recurrence-free survival curves in HCC patients who underwent HR according to MVI probability (<50% vs ≥50%) based on the model. (*C*) Overall and (*D*) recurrence-free survival curves in HCC patients who underwent LT according to MVI probability (<50% vs ≥50%) based on the model.

presented). Zhou et al[24] reported that the required minimal length of the resection margin is 6 mm to achieve 100% micrometastasis clearance in the surrounding liver tissue for HCC. Yamashita et al[25] reported that the disadvantage with the disease-free survival rate for patients with HCC with MVI could be removed by HR with a wide tumor margin of ≥5 mm. Although surgical margin is controversial, a wide surgical margin might be one effective therapy for removing the main tumor with these satellite lesions or tumor thrombi. We suggest that these concepts may even be adopted in patients within the Milan criteria because patients with a ≥50% probability had a poorer prognosis than those with a <50% probability, among patients meeting the Milan criteria. This model could therefore be used to calculate the MVI probability preoperatively, thus guiding the choice of surgical strategy.

Tumor type has been classified using CE-CT.[14,15,26,27] In this study, we classified tumor shape (boundary or nonboundary type) using CE-CT because this method was less ambiguous and a good predictor of gross classification. However, the Japanese gross classification has also been used as a prognostic factor of survival and to predict MVI.[28] Wu et al[29] reported that tumor shape reflected the incidence of MVI using various imaging techniques,[29] whereas He et al[14] also typed tumors according to shape using CE-CT and associated them with MVI, with a similar accuracy to gross classification of 65.3%.[14]

The current study has some limitations. First, it was a retrospective, single-center study. Second, numerous imaging modalities are now available for predicting MVI preoperatively, and contrast-enhanced ultrasound shows a significantly higher correlation with gross classification than CE-CT (86.9% vs 65.6%).[30] Tumor shape evaluated by gadolinium ethoxybenzyl diethylenetriamine pentaacetic acid-enhanced MRI or apparent diffusion coefficients evaluated by diffusion-weighted MRI could also be useful for predicting MVI.[7,31] The use of these imaging techniques may improve the predictive accuracy for MVI, but more experience and skill may be required to implement them.

In conclusion, we developed a predictive model for MVI in patients with HCC, suitable for use in potential candidates for either HR or LT, based on tumor size, AST, NLR, tumor boundary, and AFP. This model could be a valuable tool in helping to decide treatment strategies in HCC patients.

Acknowledgments

We would like to thank Dr. V. Cailliez and K. Murotani for statistical analyses.

Conflict of interest

The authors declare no conflict of interest.

Supplementary materials

Supplementary material associated with this article can be found, in the online version, at https://doi.org/10.1016/j.surg.2019.01.012.

References

1. Vauthey JN, Lauwers GY, Esnaola NF, et al. Simplified staging for hepatocellular carcinoma. *J Clin Oncol*. 2002;20:1527–1536.
2. Rodríguez-Perálvarez M, Luong TV, Andreana L, Meyer T, Dhillon AP, Burroughs AK. A systematic review of microvascular invasion in hepatocellular carcinoma: Diagnostic and prognostic variability. *Ann Surg Oncol*. 2013;20:325–339.
3. Mazzaferro V, Llovet JM, Miceli R, et al. Predicting survival after liver transplantation in patients with hepatocellular carcinoma beyond the Milan criteria: A retrospective, exploratory analysis. *Lancet Oncol*. 2009;10:35–43.
4. Shim JH, Jun MJ, Han S, et al. Prognostic nomograms for prediction of recurrence and survival after curative liver resection for hepatocellular carcinoma. *Ann Surg*. 2015;261:939–946.
5. Lim KC, Chow PK, Allen JC, et al. Microvascular invasion is a better predictor of tumor recurrence and overall survival following surgical resection for hepatocellular carcinoma compared to the Milan criteria. *Ann Surg*. 2011;254:108–113.
6. Shirabe K, Toshima T, Kimura K, et al. New scoring system for prediction of microvascular invasion in patients with hepatocellular carcinoma. *Liver Int*. 2014;34:937–941.
7. Suh YJ, Kim MJ, Choi JY, Park MS, Kim KW. Preoperative prediction of the microvascular invasion of hepatocellular carcinoma with diffusion-weighted imaging. *Liver Transpl*. 2012;18:1171–1178.
8. Banerjee S, Wang DS, Kim HJ, et al. A computed tomography radiogenomic biomarker predicts microvascular invasion and clinical outcomes in hepatocellular carcinoma. *Hepatology*. 2015;62:792–800.
9. Yu YQ, Wang L, Jin Y, et al. Identification of serologic biomarkers for predicting microvascular invasion in hepatocellular carcinoma. *Oncotarget*. 2016;7:16362–16371.
10. Forner A, Gilabert M, Bruix J, Raoul JL. Treatment of intermediate-stage hepatocellular carcinoma. *Nat Rev Clin Oncol*. 2014;11:525–535.
11. Llovet JM, Brú C, Bruix J. Prognosis of hepatocellular carcinoma: The BCLC staging classification. *Semin Liver Dis*. 1999;19:329–338.
12. Bruix J, Sherman M, Llovet JM, et al. Clinical management of hepatocellular carcinoma. Conclusions of the Barcelona-2000 EASL conference. European Association for the Study of the Liver. *J Hepatol*. 2001;35:421–430.
13. Adam R, Bhangui P, Vibert E, et al. Resection or transplantation for early hepatocellular carcinoma in a cirrhotic liver: Does size define the best oncological strategy? *Ann Surg*. 2012;256:883–891.
14. He J, Shi J, Fu X, et al. The clinicopathologic and prognostic significance of gross classification on solitary hepatocellular carcinoma after hepatic resection. *Medicine (Baltimore)*. 2015;94:e1331.
15. Fu X, Mao L, Tang M, et al. Gross classification of solitary small hepatocellular carcinoma on preoperative computed tomography: Prognostic significance after radiofrequency ablation. *Hepatol Res*. 2016;46:298–305.
16. Harrell Jr FE, Lee KL, Mark DB. Multivariable prognostic models: Issues in developing models, evaluating assumptions and adequacy, and measuring and reducing errors. *Stat Med*. 1996;15:361–387.
17. Janssen KJ, Donders AR, Harrell Jr FE, et al. Missing covariate data in medical research: to impute is better than to ignore. *J Clin Epidemiol*. 2010;63:721–727.
18. Cucchetti A, Piscaglia F, Grigioni AD, et al. Preoperative prediction of hepatocellular carcinoma tumour grade and micro-vascular invasion by means of artificial neural network: A pilot study. *J Hepatol*. 2010;52:880–888.
19. Duvoux C, Roudot-Thoraval F, Decaens T, et al. Liver transplantation for hepatocellular carcinoma: A model including α-fetoprotein improves the performance of Milan criteria. *Gastroenterology*. 2012;143:986–994.
20. Lei Z, Li J, Wu D, et al. Nomogram for preoperative estimation of microvascular invasion risk in hepatitis B virus-related hepatocellular carcinoma within the Milan criteria. *JAMA Surg*. 2016;151:356–363.
21. Vivarelli M, Cucchetti A, Piscaglia F, et al. Analysis of risk factors for tumor recurrence after liver transplantation for hepatocellular carcinoma: Key role of immunosuppression. *Liver Transpl*. 2005;11:497–503.
22. Bertuzzo VR, Cescon M, Ravaioli M, et al. Analysis of factors affecting recurrence of hepatocellular carcinoma after liver transplantation with a special focus on inflammation markers. *Transplantation*. 2011;91:1279–1285.
23. Halazun KJ, Tabrizian P, Najjar M, et al. Is it time to abandon the Milan criteria?: Results of a bicoastal US collaboration to redefine hepatocellular carcinoma liver transplantation selection policies. *Ann Surg*. 2018;268:690–699.
24. Zhou XP, Quan ZW, Cong WM, et al. Micrometastasis in surrounding liver and the minimal length of resection margin of primary liver cancer. *World J Gastroenterol*. 2007;13:4498–4503.
25. Yamashita Y, Tsuijita E, Takeishi K, et al. Predictors for microinvasion of small hepatocellular carcinoma $\leq$ 2 cm. *Ann Surg Oncol*. 2012;19:2027–2034.
26. Kawamura Y, Ikeda K, Hirakawa M, et al. New classification of dynamic computed tomography images predictive of malignant characteristics of hepatocellular carcinoma. *Hepatol Res*. 2010;40:1006–1014.
27. Nakayama H, Takayama T, Okubo T, et al. Proposal of objective morphological classification system for hepatocellular carcinoma using preoperative multiphase computed tomography. *J Gastroenterol*. 2014;49:1430–1437.
28. Kanai T, Hirohashi S, Upton MP, et al. Pathology of small hepatocellular carcinoma. A proposal for a new gross classification. *Cancer*. 1987;60:810–819.
29. Wu TH, Hatano E, Yamanaka K, et al. A non-smooth tumor margin on preoperative imaging predicts microvascular invasion of hepatocellular carcinoma. *Surg Today*. 2016;46:1275–1281.
30. Hatanaka K, Minami Y, Kudo M, Inoue T, Chung H, Haji S. The gross classification of hepatocellular carcinoma: Usefulness of contrast-enhanced US. *J Clin Ultrasound*. 2014;42:1–8.
31. Ariizumi S, Kitagawa K, Kotera Y, et al. A non-smooth tumor margin in the hepatobiliary phase of gadoxetic acid disodium (Gd-EOB-DTPA)-enhanced magnetic resonance imaging predicts microscopic portal vein invasion, intrahepatic metastasis, and early recurrence after hepatectomy in patients with hepatocellular carcinoma. *J Hepatobiliary Pancreat Sci*. 2011;18:575–585.